Journal of Materials Science Research; Vol. 7, No. 3; 2018
ISSN 1927-0585 E-ISSN 1927-0593
Published by Canadian Center of Science and Education

Effect of Annealing on Microstructure, Grain Growth and Hardness of Nanocrystalline Cu-Zr Alloy Prepared by Cryogenic Ball Milling

Nidhi Khobragade[1], Koushik Sikdar[1], Binod Kumar[1] & Debdas Roy[1]

[1] Department of Materials and Metallurgical Engineering, National Institute of Foundry and Forge Technology, Ranchi 834 003, India

Correspondence: Debdas Roy, Department of Materials and Metallurgical Engineering, National Institute of Foundry and Forge Technology, Ranchi 834 003, India. Tel: 91−651−229−2018. E-mail: droy2k6@gmail.com

Received: April 18, 2018 Accepted: June 8, 2018 Online Published: June 30, 2018

doi:10.5539/jmsr.v7n3p69 URL: https://doi.org/10.5539/jmsr.v7n3p69

Abstract

Nanocrystalline Cu-0.75 at.%Zr alloy was synthesized by high energy ball milling under cryogenic temperature. To investigate the influence of 0.75 at.%Zr addition on thermal stabilization of nanocrystalline state of Copper, milled powder was annealed up to $T/T_m = 0.79$ for 1h in an inert atmosphere. The microstructural changes of both milled and annealed powders were characterized by X-ray diffraction (XRD) and transmission electron microscopy (TEM). Mechanical properties were determined in terms of hardness. It was found that addition of 0.75 at.%Zr can stabilize grain size at higher temperature, i.e., ~ 32 nm at 800ºC (T/Tm = 0.79). The hardness of Cu-0.75 at.%Zr at 800ºC was found to decrease by only ~ 13% as opposed to a 65% decrease in pure copper from cryomilled condition. The thermal stability of Cu-0.75 at.%Zr system at high temperatures was attributed to the kinetic stabilization, i.e., grain boundary pinning by intermetallic phases. Thermal stability contributions were assessed by thermodynamic models elicits added Zr is not sufficient for stabilization, rather kinetic stabilization (by intermetallic pinning of grain boundary) became active at higher annealing temperature.

Keywords: Cryomilling; Nanocrystalline; X-ray diffraction; Hardness; Thermal stability

1. Introduction

Superior combination of mechanochemical properties than conventional one draws attention towards practical implementations of nanocrystalline (grain size<100 nm) materials. However, increased grain boundary energy contribution imposes inherited instability in these nanocrystallinematerials. Curvature dependent driving force for grain coarsening can be obtained in terms of pressure (P) acting on grain boundary (Humphreys & Hatherly, 2012), given as

$$P = \frac{A\gamma_0}{R_{GB}} \quad (1)$$

Where A is a constant (value close to 1), $\gamma_0$is intrinsic grain boundary energy and $R_{GB}$is the radius of curvature of grains (in order of a few nm). Hence, very high driving force invariably makes difficult retention of nanocrystallinestate especially at higher temperature where grain boundary mobility proliferates. This in turn limits its processing techniques, consolidation and operating temperature. ACombination of FCC crystal structure and high stacking fault (78 mJm^2) (Rohatgi, Vecchio, & Gray, 2001) energy makes copper an ideal material to be usedfor investigations. Coarsening of nanocrystalline pure Cu has beenreported even at room temperature (Rohatgi, Vecchio, & Gray, 2001). Established mechanisms of thermal stabilization of nanocrystalline materials include both kinetic and thermodynamic factors. In kinetic or Zener mechanism thermal migration of grain boundaries have been found to be mitigated by particle pinning and/or solute drag, reported in systems like Fe-Cr-Zr (Saber, Kotan, Koch, & Scattergood, 2012), Cu-Y (Mula et al., 2015), Cu-Al-Y (Roy et al., 2014) etc. Particle pinning pressure (P_z) on grain boundary is estimated as (Hillert, 1965)

$$P_z = \frac{3f\gamma_0}{2r_P} \quad (2)$$

Where, f , γ_0 and r_P, are volume fraction of precipitate, surface energy and precipitate radius respectively. Equation (2) indicates that smaller sized precipitates with large volume are more effective in pinning. In

thermodynamic mechanism preferential solute segregation on grain boundariesreduces the grain boundary energy of the solvent. Grain boundary energy change ($d\gamma$) is given by theGibbs interface equation as:

$$d\gamma = -\Gamma_s \, d\mu \tag{3}$$

Where Γ_s is excess solute atoms(mole/area) on grain boundaries and, μ is the chemical potential of solutes (energy/mole). Decrease in the grain boundary energy can be estimated as:

$$\gamma = \gamma_0 - \Gamma_s[\Delta H_{seg} - T\Delta S_{seg}] \tag{4}$$

Where γ_0 is intrinsic grain boundary energy, ΔH_{seg} and ΔS_{seg} are enthalpy and entropy of segregation. Normally entropy of segregation is taken equal to zero ($\Delta S_{seg} = 0$) (Darling et al., 2014) i.e. if $[\Delta H_{seg} - T\Delta S_{seg}]$<0, thengrain boundary solute segregation becomes effective in thermal stabilization.A higher elastic misfit ($\Delta H_{seg} > 0$) favors grain boundary solute segregation, reported for Pd-Zr (Krill III, Ehrhardt, & Birringer, 2005), Fe-Cr-Hf (Li et al., 2014), Fe-Zr (Darling et al., 2008) systems.A hybrid strengthening mechanism was reported for Cu-Ta system (Darling et al., 2013). Darling et al. (2008) reported that addition of 1at.%Zr in Fe retains 50nm grain size up to T/T_m=0.92 (T_m is the melting temperature). They attributed the superior thermal stability to reduction in grain boundary energy by Zr segregation. When Zr in added to Cu, the change in elastic enthalpy (ΔH_{seg}) is ~ 90.8 kj/mol (Roy et al., 2014), which is comparable with the enthalpy change when Zris added in Fe, i.e.$\Delta H_{seg} = 92\ kJ/mol$. (Darling et al., 2008). Moreover, solubility of Zrin Cu (0.12 at.% at 972°C) (Arias & Abriata, 1990) is comparable with the solubility of Zr in Fe (0.5 at.% at 1300°C) (Darling et al., 2008). Previously, Atwater, Scattergood, and Koch (2013) established that addition of 1at.%Zr in Cu retains grain size of 29.5 nm up to 900°C (T/T_m=0.87) and proposed a combined strengthening mechanism for the stability of grains at high temperature. Roy et al. (2013) added a lower Zr content of 0.5 at.% and showed that it can stabilize grain size of 35.2 nm up to 800°C.It has been shown that addition of higher Zr content in Cu causes formation of amorphous state (Xu et al., 2004). Cu is extensively used for making conductors materials. In order to design a conductor which can retain high strength at higher operation temperature we need to retain nanocrystalline microstructure. Previously, with 1 at.%Zr addition in Cu numerous intermetallic phases were formed at high temperature (say 900°C) (Atwater, Scattergood, & Koch, 2013). Hence, stabilization potential of Zr by thermodynamically controlled mode was not realized. Furthermore, a detailed thermodynamic calculation for lower (<1 at. %) concentration of Zrin Cu is not yet explored. In present work, Cu-0.75 at.% Zralloy has been prepared by the mechanical alloying route and effect of this small concentration of Zr on the thermal stabilization of the microstructure has been assessed.

2. Experimental Details

2.1 Materials and Methods

Copper (Cu)and Zirconium (Zr) powders (99.9%, Alfa Aesar) were mixed in appropriate proportion (0.75at%Zr) and put intoa stainless steel vial (440 stainless steel vial-Spex Sample Prep) for mechanical alloying. The vial was then sealed in an argon atmosphere followed by mechanical milling in Spex 8000 mixer/mill for 8 hrs at cryogenic temperature (-196 ºC). Milling media was specially designed stainless steel balls (440C SS balls) with the ball to powder weight ratio of 10:1. Milled powder was then transferred into sealed vacuum tube for subsequent annealing operation for studying property alteration of powder blend. Isochronal annealing ofthe milled powder was performed for 1hr at a temperature range of 200 to 800°C (i.e. up to T/T_m=0.79). To compare with pure copper, same process was performed with Cu powders.

2.2 Phase and Microstructure Characterization

Phase identification of both milled and annealed powder samples were performed by X-ray diffraction (XRD) analysis (PANalytical 3 kW X'pert Powder XRD –Multifunctional). XRD patterns were obtained using CuKάincident radiation with scan angle (2θ) range from 30° to 100° and with a scanning rate and step size of 0.02°/min and 0.017°, respectively. The crystallite size was determined by X-rayline broadening using the Scherrer equation (Cullity, 2001),

$$D = \frac{k\lambda}{\beta \cos\theta} \tag{5}$$

Where, D is the crystallite size, λ is the wavelength of the incident X-ray radiation (0.1541nm), k is the Scherrerconstant (= 0.94), β is the peak width at half maximum intensity (or full width half maximum, FWHM), and θ is the peak maximum position. The broadening of adiffraction peak is attributed to the synergistic contribution of both instrumental and sample condition. The instrumental broadening is corrected by subtracting the integral breadth of standard sampleusing following equation,

$$\beta = [(\beta^2)_{measured} - (\beta^2)_{standard}]^{1/2} \quad (6)$$

Microstructural characterization of the milled and annealed powders was also carried out by using transmission electron microscopy (JEOL JEM 2000FX) with beam energy of 200 keV. The milled and annealed powders were compacted at 2.6GPa pressure to form disk shaped compact for TEM investigation. The compacts were then mechanically polished to a thickness of ~100 mm followed by electropolishing (30 vol% nitric acid in methanol at -20° C).

2.3 Mechanical Properties Evolution

To evaluate the mechanical properties, milled and annealed powders were mounted on a glass slide and polished for surface finishing. Vickers microhardness measurements were performed by a minimum of 10 indents for each annealed conditions using SIMANDZU Semi-Automatic Micro Vickers hardness tester. The microhardness test was carried out using 25g load with a dwell time of 15sec for each indentation.

3. Results and Discussion

3.1 Phase and Microstructural Analysis

The XRD patterns ofmilled and annealed powders (200°C, 400°C, 600°C and 800°C) are shown in Figure 1a. The absence of Zrpeaks in Figure 1a may be attributed to the complete dissolution of Zrin Cu matrix due to mechanical milling and/or the small amount of Zr (only 0.7 at.%). It is evident that increase in annealing temperature leads to increase in intensity and decrease in width of XRD peaks. This indicates that the lattice parameter of Cu decreased with increase in annealing temperature and this might be attributed to the solute (Zr) leaving the solid solution. For detailed investigation, lattice parameter (a_{Cu}) was calculated as a function of annealing temperatures from XRD. In order to get precise values of a_{Cu} for a particular condition, calculated values from four major peaks were plotted against $cos^2\theta/\sin\theta$ to $cos\theta = 0$ (Cullity, 2001). Figure 1b shows variation in lattice parameters of milled and annealed powders (as a function of annealing temperature) against the lattice parameter of pure Cu at room temperature (a_{Cu} =0.36144 nm). Calculated lattice parameters showa rapid decrease from 0.36223nm (milled powders) to 0.36179 nm (T/T_m = 0.35 or 200°C annealed) followed by a slow decrease to 0.36171nm (at 400°C or T/T_m= 0.49), and then remain almost constant till 800°C.Following Darling et al. (2008), relative fraction of solute (Zr)in a solid solutioncan be assessed from changes in lattice parameters with respect to pure Cu as(1-f), where

$$f = \frac{a_{Cu}^{Milled} - a_{Cu}^{Annealed}}{a_{Cu}^{Annealed} - a_{Cu}^{Pure}} = 0.66$$

i.e. 0.34 of total added Zr remains in parent Cu lattice after annealing at 800°C for 1h.

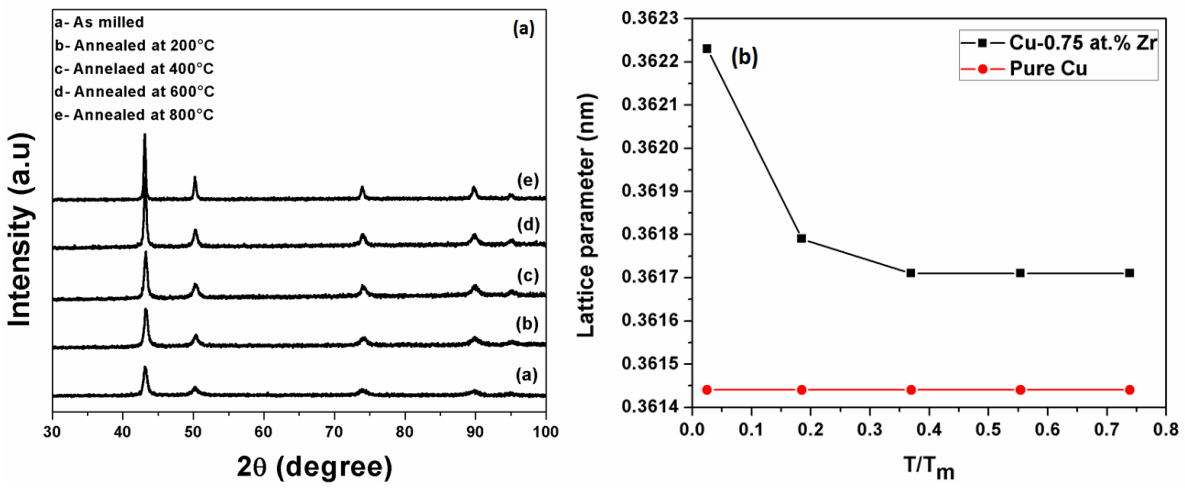

Figure 1(a) XRD patterns of $Cu_{99.25}Zr_{0.75}$ milled for 8hrs and annealed at various temperatures, (b) variation in lattice parameters with annealing temperatures

The TEM dark field (DF) image and corresponding selected area electron diffraction (SAED) of milled powder are shown in Figure 2a and 2b. A continuous diffraction ring of FCC Cu confirms formation of nanocrystalline

grain. Few bright spots on SAED rings are due to more diffraction from a particular set of the atomic plane than others due to chosen orientation of SAED plane. The TEM dark field image and SAED patternof $Cu_{99.25}Zr_{0.75}$alloy annealed at 800°C are shown in Figure 2c and 2d, respectively. Apart from the FCC Cu rings, additional rings are also visible in the SAED pattern of annealed alloy. This ringscorrespond to Cu_5Zr and the same phase has been observed in the previous studies (Atwater, Scattergood, & Koch, 2013; Roy et al., 2013). This intermetallic phase (Cu_5Zr) is shown by arrows in the dark field TEM image (Figure 2c). During annealing, the Zr solute atoms come out of the solid solution and precipitates as Cu_5Zr. Due to limited potential of XRD technique, although no detectable peaks of second phase were present in XRD patterns (Figure 1a), TEM images confirms the presence of intermetallic phases at high temperature. Furthermore, the continuous rings of Cu in the SAED pattern, confirm stability of nanocrystalline state even after annealing at high ($0.79T_m$) temperature.

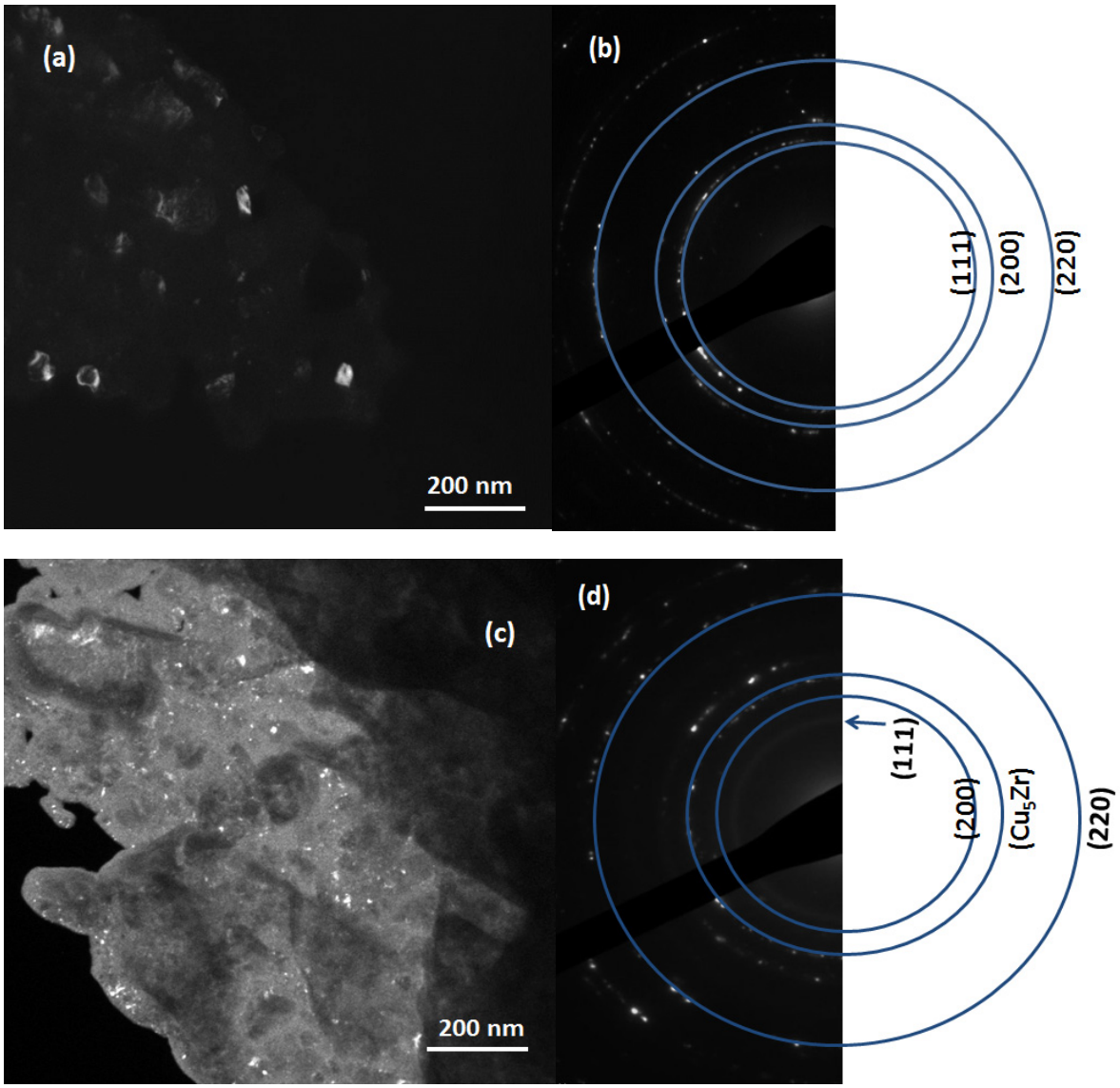

Figure 2 $Cu_{99.25}$ $Zr_{0.75}$ alloy (a),(c) dark field TEM images of milled and annealed (800°C) powder, (b) and (d) corresponding SAED patterns

3.2 Thermal Stability of Nanocrystalline Structure and Hardness

Figure 3a shows grain sizes obtained byScherrer equation with respect to normalized isochronal (1h) annealing temperature for pure Cu and $Cu_{99.25}Zr_{0.75}$. It can be seen that the both pure Cu and $Cu_{99.25}$ $Zr_{0.75}$ were nanocrystalline and had approximately same gran size after milling. However, there is a drastic increase in grain size in case of

pure Cu compared to $Cu_{99.25}Zr_{0.75}$ when annealed at 800°C. A small increase in grain size of $Cu_{99.25}Zr_{0.75}$ compared to pure Cu after annealing indicated that addition of a slight amount of Zr inhibits the grain growth, and therefore, can maintain nanocrystalline nature of the alloy. The stability of nanocrystalline nature of $Cu_{99.25}Zr_{0.75}$ even at hightemperature can be attributed to the formation of Cu_5Zr intermetallic phase at grain boundaries, which reduces the movement of grain boundaries and thereby inhibits grain growth.

Figure 3b shows room temperature Vickers microhardnessvalues vs. isochronal annealing temperature of pure Cu and the Cu–Zr alloy. The hardness values of initially milled powders of both pure Cu and $Cu_{99.25}Zr_{0.75}$ are approximately same (pure Cu~ 2.88GPa and $Cu_{99.25}Zr_{0.75}$ ~2.93 GPa). This indicates that the solid solution strengthening effect of Zr in Cu is very little due to the small content of Zr (only 0.75 at.%). The hardness values of pure Cu decrease with increase in annealing temperature (~1 GPa) at 800°C (~ 65% decrease in hardness compared to milled condition). In contrast, it is interesting to note that the hardness values of $Cu_{99.25}Zr_{0.75}$ remain almost constant till annealing temperature of 600°C, however, there is a slight decreases in the hardness value when annealed at 800°C compared to milled condition (~13% decrease). Moreover, the harness of $Cu_{99.25}Zr_{0.75}$ always remains higher than pure Cu at all annealing temperature. This relative decrease in hardness values can be correlated to the relative increase in grain size (Figure 3a) as well as effect of dispersion strengthening by the presence of Cu_5Zr intermetallic phases. The dramatic decrease in hardness of pure Cu is related to the excessive grain coarsening with increase in annealing temperature, as shown in Figure 3a. The static hardness values of $Cu_{99.25}Zr_{0.75}$ till 800°C can be attributed to grain boundary pinning by intermetallic particles, which nullifies the effect of slight increase in grain size. Although, the grain size measurements were performed using XRD data rather than the actual microstructure, grain size calculations from X-ray peak broadening has been found to be accurate even below 40 nm (Roy et al., 2014).

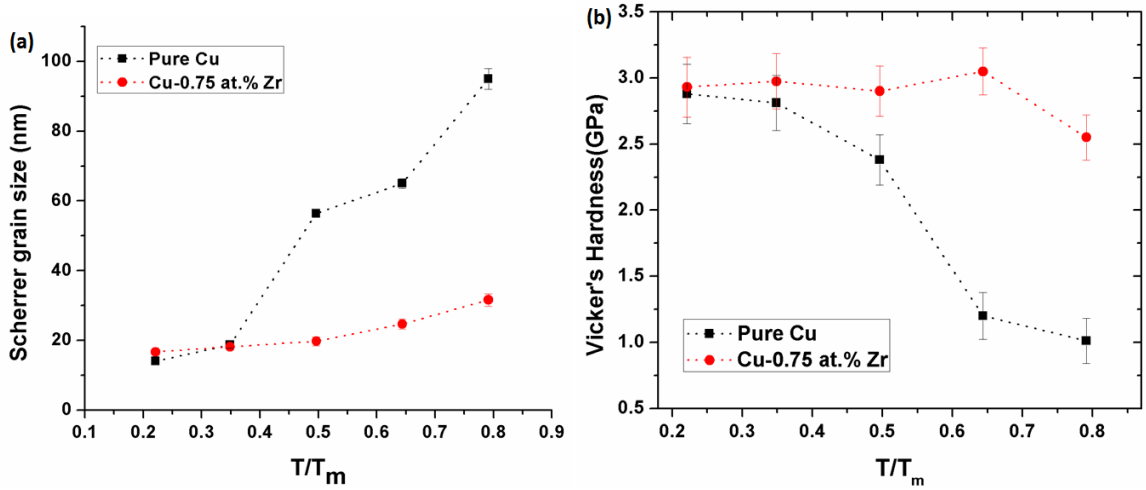

Figure 3. (a) The Scherrer grain size and (b) Vickers hardness vs. normalized isochronal annealing temperature for pure Cu and Cu-0.75at.%Zr

The change in grain boundary energy owing to solute segregation can be calculated from equation (6), by considering $\Delta S_{seg}=0$ as:

$$\gamma = \gamma_0 - \Gamma_s \Delta H_{seg} \tag{7}$$

Where γ is the reduced grain boundary energy due to solute (Zr) addition, γ_0 is intrinsic grain boundary energy, Γ_s is excess solute atoms (mol./area) on grain boundaries, ΔH_{seg} is the enthalpy change due to grain boundary solute segregation. Further, equation 7 can be expressed in terms of normalized grain boundary energy as Atwater, Scattergood, and Koch (2013).

$$\frac{\gamma}{\gamma_0} = 1 - \Gamma_s \frac{\Delta H_{seg}}{\gamma_0} \tag{8}$$

Where, $\Gamma_s = 2(X_A^{gb} - X_A^b)/\sigma$

Here X_A^{gb} is the grain boundary solute content (in mole), X_A^b is the solute concentration within the grain and σ is the molar grain boundary area. Complete thermodynamic stabilization by grain boundary segregation as discussed in Darling et al. (2013) is obtained when normalized grain boundary energy (γ/γ_0) equals with zero and the correspondingX_{Zr}^{Gb} is minimum solute content for stabilization.The free surface segregation energyin terms of chemical and elastic effects is given by the classical Wynblatt and Ku bilayer grain boundary model (WK model) (Wynblatt & Ku, 1977; Wynblatt & Chatain, 2006)

$$\Delta H_{seg} = \Delta H_{chem} - \Delta E_{el} \tag{9}$$

$$\Delta H_{chem} = (\sigma\gamma_A - \sigma\gamma_B)(1 - \alpha) - \frac{8\Delta H_m}{Z}\left[z_l\left(X_A^{gb} - X_A^b\right) - z_v(X_A^b - 0.5) + z_v\alpha(X_A^{gb} - 0.5)\right] \tag{10}$$

Where,

$$\Delta E_{el} = -\frac{24\pi KGr_A r_B(r_0 - r_1)^2}{3Kr_B + 4Gr_A}$$

Where, A and B are the solute and solvent atoms respectively, γ_A and $\gamma_B$are the surface free energies, α is the ratio of interface and bulk bond strengths, (α = 5/6) (Darling, VanLeeuwen, Koch, & Scattergood, 2010), σ is the molar area for solvent, ΔH_m is the enthalpy of mixing of equimolar liquid A and B, Z_c(=12) is the coordination number ($Z_c = z_l + 2z_v$), $z_l(=6)$ is the number of in plane bonds and $z_v(=3)$ is half of the number of out plane bonds, X_A^{gb} and X_A^b are the mole fractions of solute on grain boundaries and in the bulk respectively and $\Delta E_{elastic}$is the elastic enthalpy. Values required for numerical estimation of grain boundary energy change due to dopant addition are given in table 1.

Table 1. Required numerical values for altered grain boundary energy calculation (Atwater, Scattergood, & Koch, 2013)

Parameters	Cu	Zr
Surface energy γ (J/m^2)	1.8075	1.9545
Molar grain boundary area σ(m^2/mole)	31,224.34	49,286.31
Atomic volume V(m^3/atom)	1.18x10^{-29}	2.34x10^{-29}
Bulk Modulus, K (GPa)	137.8	89.8
Shear Modulus, G(GPa)	48.3	35

Using the values given in the table 1 and bilayer grain boundary model (i.e. WK model), the variation of grain boundary energy with solute concentration is plotted in Figure 4. It is evident from Figure 4 that the required solute content for zero grain boundary energy is very small. i.e. 0.14 mole Zr.

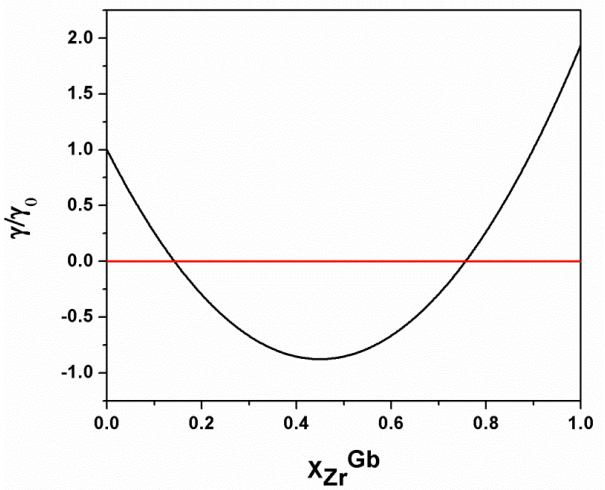

Figure 4 Grain boundary energy variation withZr solute concentration

As grain size increases, the grain boundary area fraction decreases, and therefore, requirement of solute with also decrease. Therefore, incorporation of grain size is required in the classical WK model. The atomic fraction of solute (f_{Zr}) for monolayer configuration is given by Darling et al. (2008)

$$f_{Zr} = 1 \Big/ 1 + \frac{v_{Zr}^{2/3}}{3v_{Cu}}\, d = 1 \Big/ 1 + 3.126\, d_G \tag{11}$$

Using $v_{Zr} = 0.0233nm^3$ and $v_{Cu} = 0.0087nm^3$ and $d_G$is grain size. However, solute excess for grain boundary monolayer (ML) configuration is independent of grain size (Darling et al., 2008), can be obtained by

$$\Gamma_{ML} = 1/2 v_{Zr}^{2/3} N_{AVG} = 1 \times 10^{-5} mol\, m^{-2} \tag{12}$$

The reduced grain boundary energy for Zr monolayer obtained as discussed in Darling et al. (2008)

$$\gamma = \left(\gamma_0 - \Gamma_{ML} H_{seg}\right) = 0.603 - 0.908 = -0.31\, J/m^2 \tag{13}$$

0.603/0.908=0.66 fraction of Zr can form a monolayer and would be sufficient for stabilization ($\gamma = 0$). For stabilizing $d = 31.6\, nm f_{Zr} = 0.01$ at.% Zr $0.01 \times 0.66 = 0.007\, at.\%$ Zr is enough for complete thermal stabilization. XRD analysis of annealed powder shows 0.34 of total Zr retains in solid solution i.e. 0.34 ×0.75=0.26 at.% Zr. It implies in principle added Zr (0.75 at.%) is sufficient for thermal stabilization by forming grain boundary monolayer.Owing to a negative heat of mixing (Abe, Shimono, Ode, & Onodera, 2006), numerous intermetallic phases (Arias & Abriata, 1990; Okamoto, 2008) exists in Cu-Zr system. It has been reported that with formation of intermetallic phases stabilization mechanism is dictated by kinetically controlled mode (Atwater, Scattergood, & Koch, 2013). Moreover, if the added Zr content below the critical requirement for thermodynamic stabilizer can disruptthe microstructure (Koch et al., 2008). Identified stable intermetallics are mainly Cu_5Zr (Atwater, Scattergood, & Koch, 2013; Roy et al., 2013; Neishi, Horita, & Langdon, 2003; Amouyal, Divinski, Estrin, & Rabkin, 2007), Cu_9Zr_2 (Muramatsu, Kimura, & Inoue, 2012). Stoichiometrically Cu_5Zr requires 16.6 at.%Zr (Atwater, Scattergood, & Koch, 2013) and Cu_9Zr_2 18.8 at.%Zr (Arias & Abriata, 1990). This signifies intermetallic formation significantly reduce global Zr concentration. Hence, then Zr mediate the stabilization mode toward kinetic mode instead.

Since Vickers hardness is related to the yield strength of material by H/σ=3, an analogous Hall-Petch equation for hardness can be formulated as, $H = H_0 + kd^{-1/2}$ (Nagumo, & Umemoto, 1997). If change in hardness after annealing is completely grain size dependent then the ratio of H_2/H_1 , ($H_2$and H_1 arehardness values after and before annealing, respectively) should be equal to $\sqrt{d_{G1}/d_{G2}}$, , where d_{G1} and d_{G2} are grain sizes in as milled and annealed condition respectively. At T/T_m=0.79, the values of $H_2/H_1$and $\sqrt{d_{G1}/d_{G2}}$,, are 0.87 and 0.73 respectively. This indicates that another strengthening mechanism is also contributing apart from Hall-Petch strengthening. The volume fraction (f) of second phase particles (Cu_5Zr) can be calculated from grain size (R= 31.6 nm) and particle size (r_P= 3.7nm) both obtained from TEM images of 800°C annealed sample as (Doherty, 2012):

$$f = \frac{0.2 r_P}{R} \tag{14}$$

The calculated volume fraction of second phase particles is ~2.34%. Inter particle spacing (λ)can be calculated from the following equation (Redsten, Klier, Brown, & Dunand, 1995):

$$\lambda = d_p\, [(\tfrac{\pi}{4f})^{1/2} - 1] \tag{15}$$

Considering that the total hardness (H) is a combination of effects from grain boundary strengthening (Hall-Petch, H_{H-P}) and particle strengthening (Orowan, H_{Oro}), the total hardness can be expressed as Atwater, Scattergood, and Koch (2013)

$$H = H_{Oro} + H_{H-P} = 3\sqrt{3}\frac{Gb}{\lambda}\frac{\ln\left(\frac{\lambda}{r_d}\right)}{2\pi}\left[\frac{\ln\left(\frac{d_P}{r_d}\right)}{\ln\left(\frac{\lambda}{r_d}\right)}\right]^{3/2} + 3[\sigma_o + k/\sqrt{d_G}] \tag{16}$$

Where G is the shear modulus of Cu (42 GPa), b is the Burger's vector (0.25 nm), $r_d$is the dislocation core radius (r_d=b) (Atwater, Scattergood, & Koch, 2013), d is the grain size, $\sigma_o$is the frictional stress (25.5 MPa), k is the Hall-Petch slope ($0.11MN/m^{3/2}$). From the aforementioned valuesH_{Oro}, H_{H-P} and H values can be calculated as0.69 GPa, 1.93 GPa and 2.62 GPa respectively. The theoretical value of 2.61 GPa is very close to the

experimentally obtained hardness value (2.61 GPa) obtained at 800°C for$Cu_{99.25}Zr_{0.75}$ alloy. Thisindicates that the hardness of $Cu_{99.25}Zr_{0.75}$ can be attributed to both grain boundary strengthening (~26%) and particle strengthening (~74%). The contribution from solid solution can be neglected as the initial hardness of the pure Cu and $Cu_{99.25}Zr_{0.75}$ alloy is approximately same. Based on above discussion it is evident that at higher annealing temperature kinetic pinning by intermetallic is governing strengthening mechanism. This can be verified by comparing experimentally observed grain size with the theoretically estimated one. According to Zener pinning modellimiting grain size can be calculated as (Manohar, Ferry, & Chandra, 1998)

$$\frac{D}{d_P} = \frac{Z}{f^m} \tag{17}$$

$d_P = 7.4\,nm$, for $f < 0.05,\ m = 0.33$ (Manohar, Ferry, & Chandra, 1998) and Z(constant=4/3), equation (17) yields grain size D=34.06 nm. The closure agreement between kinetically stabilize grain size (34.06 nm) and experimentally observed grain size (32 nm) elicits kinetic stabilization is operative thermal stabilization mechanismin Cu-0.75 at.%Zr system.

4. Conclusions

Present findings prescribe a possible route for preparing and retaining high strength of Cu at higher operating temperature. Addition of 0.75 at.%Zr results in stability of nanocrysalline state of copper at higher temperature (up to 800ºC). A decrease of only 13% (or 16%) was observed in the case of Cu-0.75 at.%Zr when annealed at 800ºC compared to cryomilled condition. Employing the modified Wynblatt–Ku, and grain size dependent monolayer model suggests added Zr can stabilize nanocrystalline Cu in thermodynamic controlled mode. However, formation of intermetallic phases excludes possibility of thermodynamically controlled stabilization. TEM investigation of annealed sample shows formation of numerous of Cu_5Zr intermetallic phase. Good agreement between experimentally obtained grain size and hardness value with the Zener predicted limiting grain size and theoretically predicted hardness values, considering the influence of intermetallic phases, suggests that the high temperature thermal stabilization of Cu- 0.75 at.%Zr is dictated mainly by Zener pinning mechanism.

Acknowledgement

Authors are grateful to Professor Carl C Koch, NCSU, Raleigh for providing needful research facilities and valuable suggestions. The work was sponsored by the Indo-US Science and Technology Forum, Govt. of India, under the grant of Indo-US fellowship No IUSSTF Fellowship/2011/ 8 dated 17/3/2011

References

Abe, T., Shimono, M., Ode, M., & Onodera, H. (2006). Thermodynamic modeling of the undercooled liquid in the Cu–Zr system. *Acta materialia, 54*(4), 909-915.

Amouyal, Y., Divinski, S. V., Estrin, Y., & Rabkin, E. (2007). Short-circuit diffusion in an ultrafine-grained copper–zirconium alloy produced by equal channel angular pressing. *Acta Materialia, 55*(17), 5968-5979.

Arias, D., & Abriata, J. P. (1990). Cu-Zr (copper-zirconium). *Journal of Phase Equilibria, 11*(5), 452-459.

Atwater, M. A., Scattergood, R. O., & Koch, C. C. (2013). The stabilization of nanocrystalline copper by zirconium. *Materials Science and Engineering: A, 559*, 250-256.

Cullity, B. D. (2001). *Elements of X-ray Diffraction*. Prentice Hall.

Darling, K. A., Chan, R. N., Wong, P. Z., Semones, J. E., Scattergood, R. O., & Koch, C. C. (2008). Grain-size stabilization in nanocrystalline FeZr alloys. *Scripta Materialia, 59*(5), 530-533.

Darling, K. A., Roberts, A. J., Mishin, Y., Mathaudhu, S. N., & Kecskes, L. J. (2013). Grain size stabilization of nanocrystalline copper at high temperatures by alloying with tantalum. *Journal of Alloys and Compounds, 573*, 142-150.

Darling, K. A., Tschopp, M. A., VanLeeuwen, B. K., Atwater, M. A., & Liu, Z. K. (2014). Mitigating grain growth in binary nanocrystalline alloys through solute selection based on thermodynamic stability maps. *Computational Materials Science, 84*, 255-266.

Darling, K. A., VanLeeuwen, B. K., Koch, C. C., & Scattergood, R. O. (2010). Thermal stability of nanocrystalline Fe–Zr alloys. *Materials Science and Engineering: A, 527*(15), 3572-3580.

Doherty, R. D. (2012). Grain Coarsening–Insights from Curvature Modeling Cyril Stanley Smith Lecture. In *Materials Science Forum* (Vol. 715, pp. 1-12). Trans Tech Publications.

Hillert, M. (1965). On the theory of normal and abnormal grain growth. *Acta metallurgica, 13*(3), 227-238.

Humphreys, F. J., & Hatherly, M. (2012). *Recrystallization and related annealing phenomena*. Elsevier, Oxford (1995), 284.

Koch, C. C., Scattergood, R. O., Darling, K. A., & Semones, J. E. (2008). Stabilization of nanocrystalline grain sizes by solute additions. *Journal of Materials Science, 43*(23-24), 7264-7272.

Krill III, C. E., Ehrhardt, H., & Birringer, R. (2005). Thermodynamic stabilization of nanocrystallinity. *Zeitschrift für Metallkunde, 96*(10), 1134-1141.

Li, L., Saber, M., Xu, W., Zhu, Y., Koch, C. C., & Scattergood, R. O. (2014). High-temperature grain size stabilization of nanocrystalline Fe–Cr alloys with Hf additions. *Materials Science and Engineering: A, 613*, 289-295.

Lu, L., Tao, N. R., Wang, L. B., Ding, B. Z., & Lu, K. (2001). Grain growth and strain release in nanocrystalline copper. *Journal of Applied Physics, 89*(11), 6408-6414.

Manohar, P. A., Ferry, M., & Chandra, T. (1998). Five decades of the Zener equation. *ISIJ international, 38*(9), 913-924.

Mula, S., Setman, D., Youssef, K., Scattergood, R. O., & Koch, C. C. (2015). Structural evolution of $Cu_{(1-X)}$ YX alloys prepared by mechanical alloying: Their thermal stability and mechanical properties. *Journal of Alloys and Compounds, 627*, 108-116.

Muramatsu, N., Kimura, H., & Inoue, A. (2012). Development and Microstructure of Cu–Zr Alloy Wire with Ultimate Tensile Strength of 2.2 GPa. *Materials Transactions, 53*(6), 1062-1068.

Nagumo, M., & Umemoto, M. (1997). The Hall-Petch relationship in nanocrystalline materials. *Materials Transactions, JIM, 38*(12), 1033-1039.

Neishi, K., Horita, Z., & Langdon, T. G. (2003). Achieving superplasticity in ultrafine-grained copper: influence of Zn and Zr additions. *Materials Science and Engineering: A, 352*(1-2), 129-135.

Okamoto, H. (2008). Cu-Zr (copper-zirconium). *Journal of phase equilibria and diffusion, 29*(2), 204-204.

Redsten, A. M., Klier, E. M., Brown, A. M., & Dunand, D. C. (1995). Mechanical properties and microstructure of cast oxide-dispersion-strengthened aluminum. *Materials Science and Engineering: A, 201*(1-2), 88-102.

Rohatgi, A., Vecchio, K. S., & Gray, G. T. (2001). The influence of stacking fault energy on the mechanical behavior of Cu and Cu-Al alloys: deformation twinning, work hardening, and dynamic recovery. *Metallurgical and Materials Transactions A, 32*(1), 135-145.

Roy, D., Atwater, M. A., Youssef, K., Ledford, J. C., Scattergood, R. O., & Koch, C. C. (2013). Studies on thermal stability, mechanical and electrical properties of nano crystalline $Cu_{99.5}Zr_{0.5}$ alloy. *Journal of alloys and compounds, 558*, 44-49.

Roy, D., Mahesh, B. V., Atwater, M. A., Chan, T. E., Scattergood, R. O., & Koch, C. C. (2014). Grain size stability and hardness in nanocrystalline Cu–Al–Zr and Cu–Al–Y alloys. *Materials Science and Engineering: A, 598*, 217-223.

Saber, M., Kotan, H., Koch, C. C., & Scattergood, R. O. (2012). Thermal stability of nanocrystalline Fe–Cr alloys with Zr additions. *Materials Science and Engineering: A, 556*, 664-670.

Wynblatt, P., & Chatain, D. (2006). Anisotropy of segregation at grain boundaries and surfaces. *Metallurgical and Materials Transactions A, 37*(9), 2595-2620.

Wynblatt, P., & Ku, R. C. (1977). Surface energy and solute strain energy effects in surface segregation. *Surface Science, 65*(2), 511-531.

Xu, D., Lohwongwatana, B., Duan, G., Johnson, W. L., & Garland, C. (2004). Bulk metallic glass formation in binary Cu-rich alloy series – $Cu_{100-x}Zr_x$ (x = 34, 36, 38.2, 40 at.%) and mechanical properties of bulk $Cu_{64}Zr_{36}$ glass. *Acta Materialia, 52*(9), 2621-2624.